

See discussions, stats, and author profiles for this publication at: <https://www.researchgate.net/publication/227164403>

# Benzothiazoles: Search for anticancer agents

ARTICLE *in* EUROPEAN JOURNAL OF MEDICINAL CHEMISTRY · MAY 2012

Impact Factor: 3.45 · DOI: 10.1016/j.ejmech.2012.05.028 · Source: PubMed

---

CITATIONS

23

---

READS

161

## 3 AUTHORS, INCLUDING:



[Malleshappa N Noolvi](#)

Shree Dhanvantary Pharmacy College

45 PUBLICATIONS 509 CITATIONS

[SEE PROFILE](#)



Benzothiazole type compounds have attracted considerable attention to anticancer research [4–14], and several attempts were made for modifying the benzothiazole nucleus to improve their antitumor activities. Modifications on the benzothiazole nucleus have resulted in a large number of compounds having diverse pharmacological activities. Among them imidazo benzothiazoles as well as polymerized benzothiazoles and other substituted benzothiazoles such as 2-(3,4-dimethoxyphenyl)-5-fluorobenzothiazole (PMX 610) (Fig. 1) has been shown to exhibit exquisitely potent ( $GI_{50} < 0.1$  nM) and selective *in vitro* antitumor properties in human cancer cell lines (e.g., colon, non small – cell lung and breast subpanels) of the National Cancer Institute (NCI) 60 human cancer cell line screen [15] and also exhibited remarkable antitumor activity against malignant cell lines [16]. 2-(4-aminophenyl)-benzothiazole (CJM 126) and its analogs comprise a novel mechanistic class of antitumor agents [17,18]. These nucleuses come from the related structure polyhydroxylated 2-phenylbenzothiazoles, flavone quercetin and the isoflavone genistein, which are tyrosine kinase inhibitors bearing potent antitumor activity [19,20]. The isoflavone, genistein [21] and the flavone, quercetin [22] are competitive inhibitors at the ATP-binding site of kinases [23,24]. As the crystal structure of 5,6-dimethoxy-2-(4-methoxyphenyl)benzothiazole was solved [20], the preliminary analysis based on comparisons between polyhydroxylated 2-phenylbenzothiazoles and the adenine fragment of ATP suggested that suitably substituted benzothiazoles might mimic the ATP competitive binding of genistein and quercetin at tyrosine kinases.

Hence in continuation of our efforts on the design and synthesis of novel anti-cancer agents [25–29] and keeping in mind the

medicinal importance of benzothiazole moiety, we synthesized and *in vitro* evaluated benzothiazoles at National Cancer Institute (NCI-USA) for anti-tumor activity. We have also tried to dock the synthesized compounds with the crystal structure of EGFR to explore the possible anticancer mechanism of our compounds. Prior compounds have been reported [30,31] to compare the anti-cancer activity of such compounds.

## 2. Rational and design

Benzothiazoles act via competing with ATP for binding at the catalytic domain of tyrosine kinase [20]. The ATP binding site has the following features; Adenine region – contains two key Hydrogen bonds formed by the interaction of N-1 and N-6 amino group of the adenine ring. Many potent inhibitors use one of these Hydrogen bonds. Sugar region – a hydrophilic region, except a few e.g. EGFR. Hydrophobic pocket – though not used by ATP but plays an important role in inhibitor selectivity. Hydrophobic channels – it is not used by ATP and may be exploited for inhibitor specificity. Phosphate binding region – This is used for improving inhibitor selectivity [32].

In this study, we present a new sub-family of compounds containing 2-anilino benzothiazole core as EGFR inhibitors. Our strategy is directed toward designing a variety of ligands which are structurally similar with basic skeleton, 4-anilino quinazoline of tinibs (erlotinib, lapatinib, gefitinib and canaratinib) with diverse chemical properties (Fig. 2). We replaced quinazoline ring with benzothiazole since both are isosteric with adenine portion of ATP

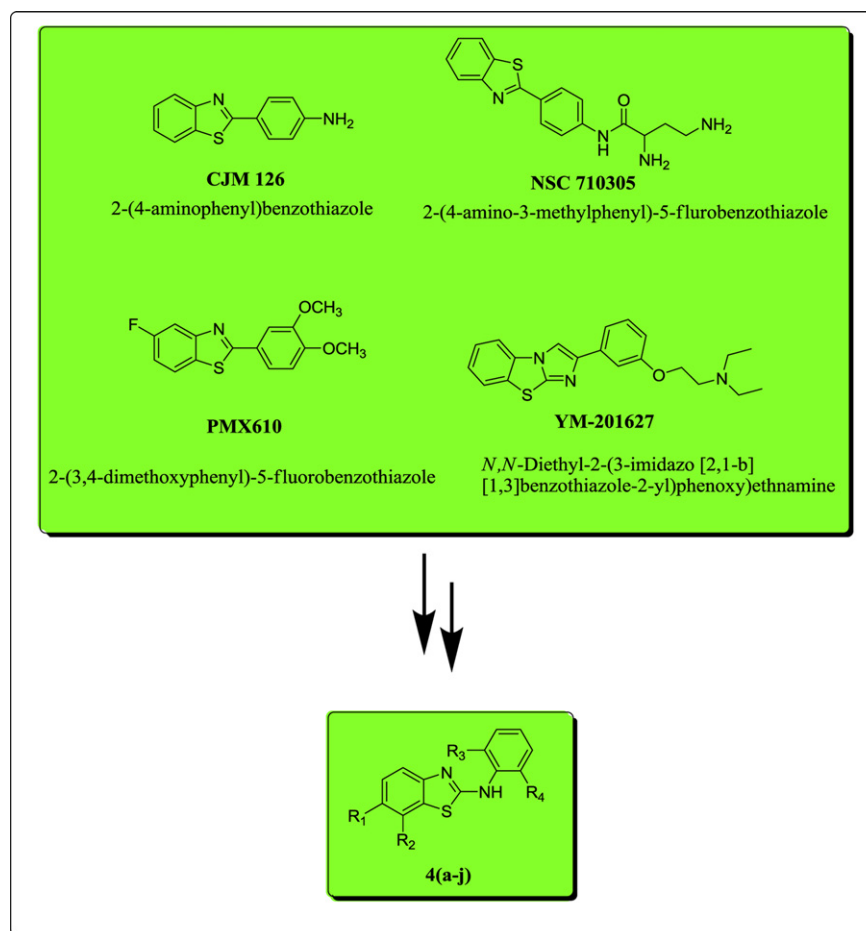
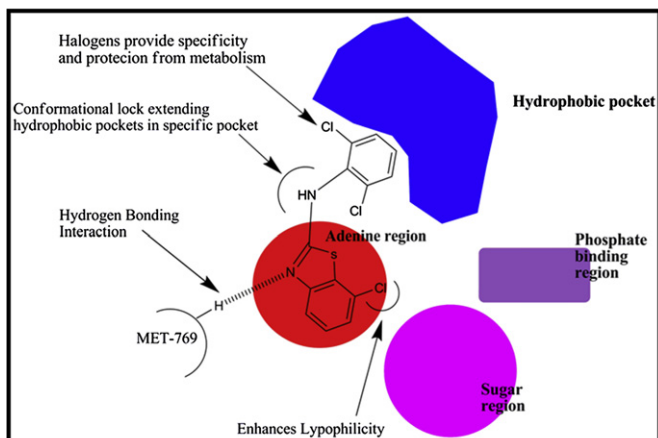
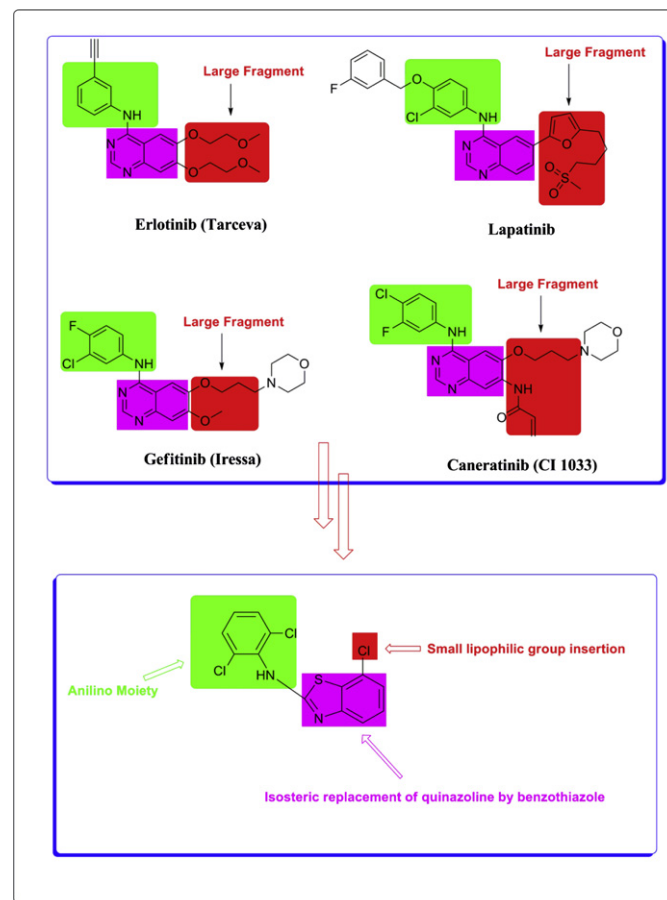


Fig. 1. Reported and proposed antitumor benzothiazole derivatives.



**Fig. 2.** Proposed hypothetical model of the highly active 7-chloro-N-(2,6-dichlorophenyl)benzo[d]thiazol-2-amine (**4i**) bound to ATP binding site of EGFR protein tyrosine kinase.

and can mimic the ATP competitive binding regions of EGFR tyrosine kinase. Like 4-aniline group in tinibs (erlotinib, lapatinib, gefitinib and canaratinib) we introduced substituted aniline ring at 2nd position of benzothiazole since secondary amino group at 2nd position of benzothiazoles is acting as conformational lock and extending substituted aniline portion into the hydrophobic pockets of EGFR – tyrosine kinase, making predominantly hydrophobic



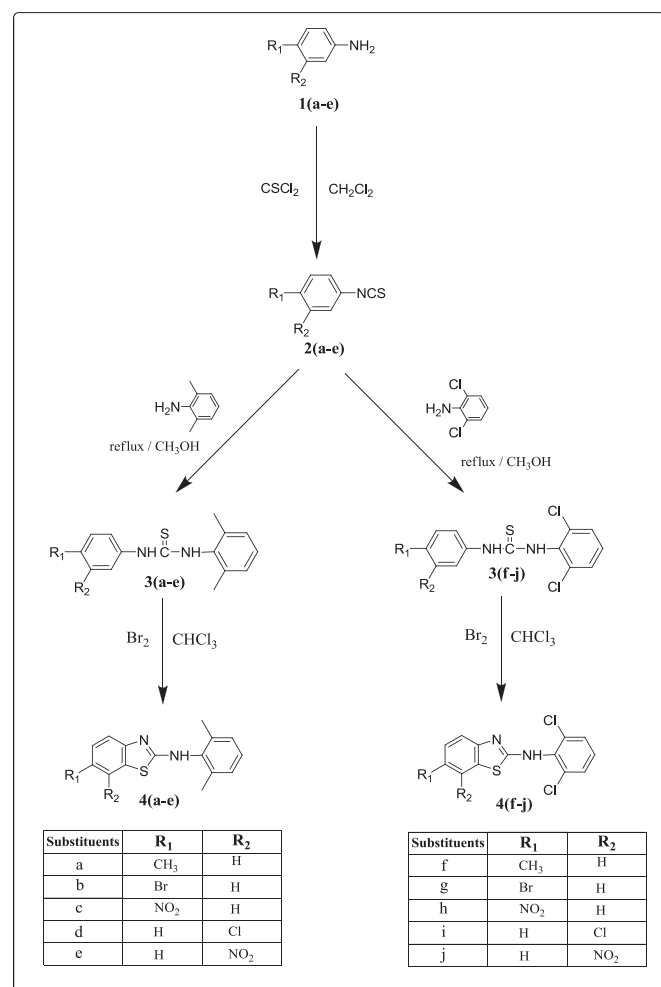
**Fig. 3.** Rational designing of proposed compounds based upon known EGFR-Tyrosine kinase inhibitor.

interactions with the protein mimicking the 3'-chloro-4'-(3-fluorobenzyl) oxy] aniline group of lapatinib (Fig. 3). We put both electron withdrawing (Cl) and electron donating ( $\text{CH}_3$ ) anilines at 2nd position just to check the effect of these substituents over anticancer activity since it is well known that presence of electron withdrawing group on anilines provides protection from metabolism and provides specificity to the molecules.

### 3. Chemistry

In Scheme 1 the compounds were synthesized using various isothiocyanates **2(a–e)**, which was prepared from different aromatic primary amines **1(a–e)** [33]. Prepared isothiocyanates **2(a–e)** yielded thioureas **3 (a–e)** on condensation with 2,6-dimethyl and 2,6-dichloro aniline [25]. Oxidative cyclization of **3 (a–e)** by bromine resulted in the synthesis of proposed compounds **4 (a–j)**. Physical data of the synthesized compound is given in Table 1.

The derivatives were characterized by spectral studies using IR,  $^1\text{H}$  NMR,  $^{13}\text{C}$  NMR and HRMS. The structures of thiocyanates were confirmed through the following spectral data **2(a–e)**. IR absorption peak at  $\sim 2200\text{--}2000\text{ cm}^{-1}$  corresponding to  $-\text{SCN}$  and  $^1\text{H}$  NMR showing a  $\sim \delta$  6.80–7.90 ppm for aromatic protons of isothiocyanates **2 (a–e)**. Thioureas **3 (a–j)** were confirmed by the absence of characteristic IR absorption peak at  $\sim 2200\text{--}2000\text{ cm}^{-1}$



**Scheme 1.**



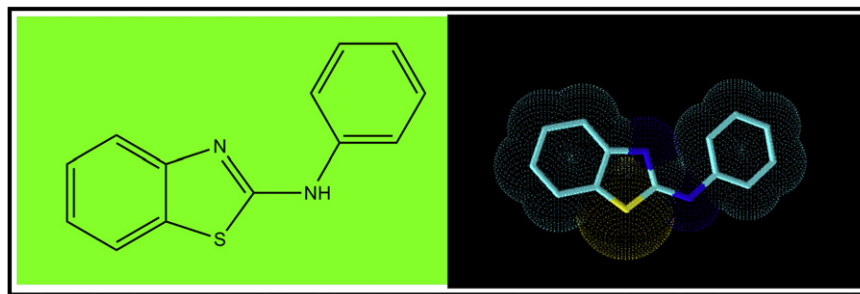


**Fig. 4.** 2D and 3D view of 2-anilino benzothiazole template used for pharmacophoric mapping alignment.

95% air and 100% relative humidity for 24 h prior to addition of experimental drugs.

After 24 h, two plates of each cell line are fixed *in situ* with TCA, to represent a measurement of the cell population for each cell line at the time of drug addition (Tz). Experimental drugs are solubilized in dimethyl sulfoxide at 400 fold the desired final maximum test concentration and stored frozen prior to use. At the time of drug addition, an aliquot of frozen concentrate is thawed and diluted to twice the desired final maximum test concentration with complete medium containing 50 µg/ml gentamicin. Additional four, 10-fold or ½ log serial dilutions are made to provide a total of five drug concentrations plus control. Aliquots of 100 µL of these different drug dilutions are added to the appropriate microtiter wells already containing 100 µL of medium, resulting in the required final drug concentrations.

Following drug addition, the plates are incubated for an additional 48 h at 37 °C, 5% CO<sub>2</sub>, 95% air, and 100% relative humidity. For adherent cells, the assay is terminated by the addition of cold TCA. Cells are fixed *in situ* by the gentle addition of 50 µL of cold 50% (w/v) TCA (final concentration, 10% TCA) and incubated for 60 min at 4 °C. The supernatant is discarded, and the plates are washed five times with tap water and air dried. Sulforhodamine B (SRB) solution (100 µL) at 0.4% (w/v) in 1% acetic acid is added to each well, and plates are incubated for 10 min at room temperature. After staining, unbound dye is removed by washing five times

with 1% acetic acid and the plates are air dried. Bound stain is subsequently solubilized with 10 mM trizma base, and the absorbance is read on an automated plate reader at a wavelength of 515 nm. For suspension cells, the methodology is the same except that the assay is terminated by fixing settled cells at the bottom of the wells by gently adding 50 µL of 80% TCA (final concentration, 16% TCA). Using the seven absorbance measurements [time zero, (Tz), control growth, (C), and test growth in the presence of drug at the five concentration levels (Ti)], the percentage growth is calculated at each of the drug concentrations levels. Percentage growth inhibition is calculated as:

$$[(Ti - Tz)/(C - Tz)] \times 100 \text{ for concentrations for which } Ti > Tz$$

$$[(Ti - Tz)/Tz] \times 100 \text{ for concentrations for which } Ti < Tz.$$

Three dose response parameters are calculated for each experimental agent. Growth inhibition of 50% (GI<sub>50</sub>) is calculated from  $[(Ti - Tz)/(C - Tz)] \times 100 = 50$ , which is the drug concentration resulting in a 50% reduction in the net protein increase (as measured by SRB staining) in control cells during the drug incubation. The drug concentration resulting in total growth inhibition (TGI) is calculated from  $Ti = Tz$ . The LC<sub>50</sub> (concentration of drug resulting in a 50% reduction in the measured protein at the end of the drug treatment as compared to that at the beginning) indicating

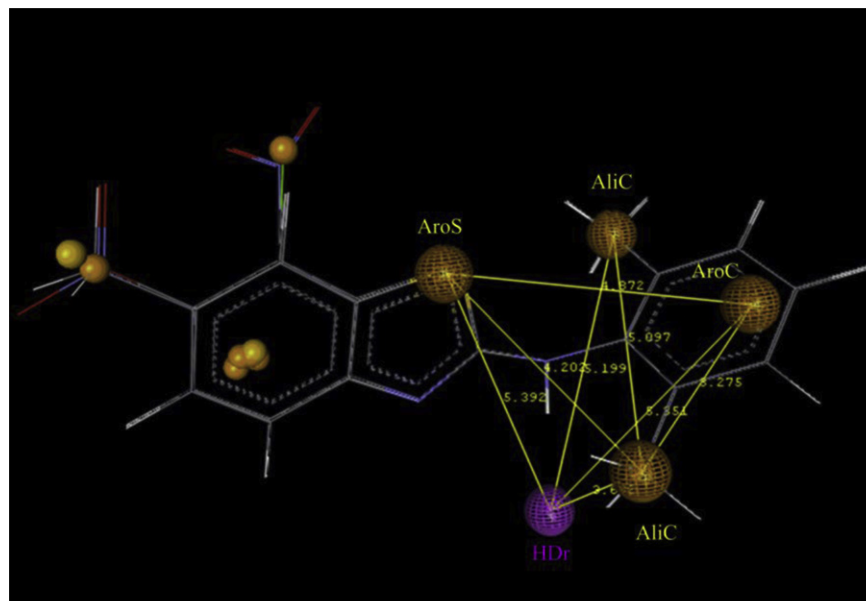


**Fig. 5.** Common biopharmacophore of 4(a–j).

a net loss of cells following treatment is calculated from  $[(Ti-Tz)/Tz] \times 100 = -50$ . Values are calculated for each of these three parameters if the level of activity is reached; however, if the effect is not reached or is exceeded, the value for that parameter is expressed as greater or less than the maximum or minimum concentration tested [34–36].

## 5. Pharmacophore mapping

A pharmacophore is the ensemble of steric and electronic features that is necessary to ensure the optimal supramolecular interactions with a specific biological targets and to trigger (or to block) its biological response. 3D pharmacophore modeling is

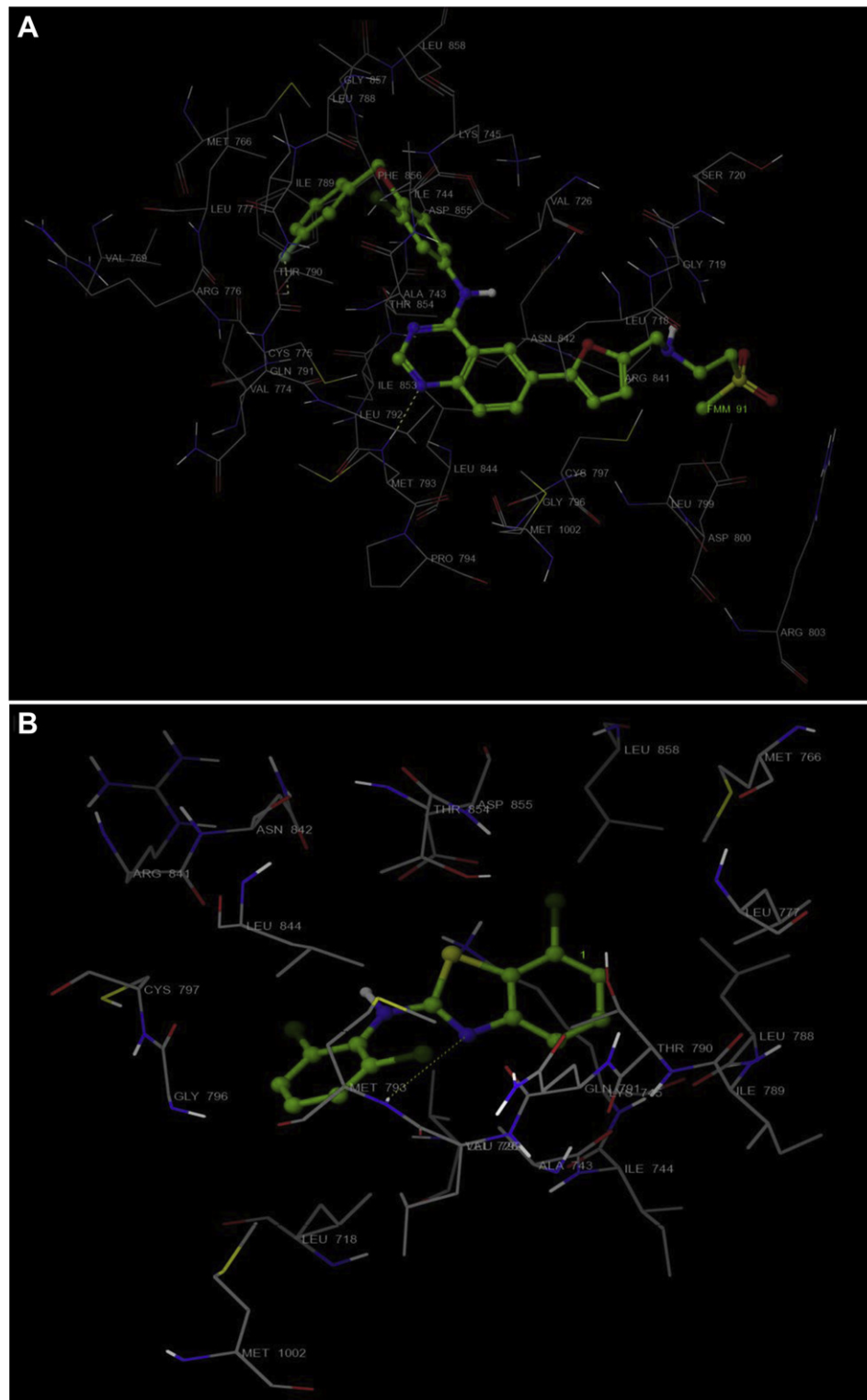


**Fig. 6.** Binding mode of **Lapatinib** (A) and compound **4i** (B) in the ATP binding site of EGFR-TK showing H bonds between N-1 of quinazoline (**Lapatinib**) and N-3 of benzothiazole (**4i**) with Met 793.

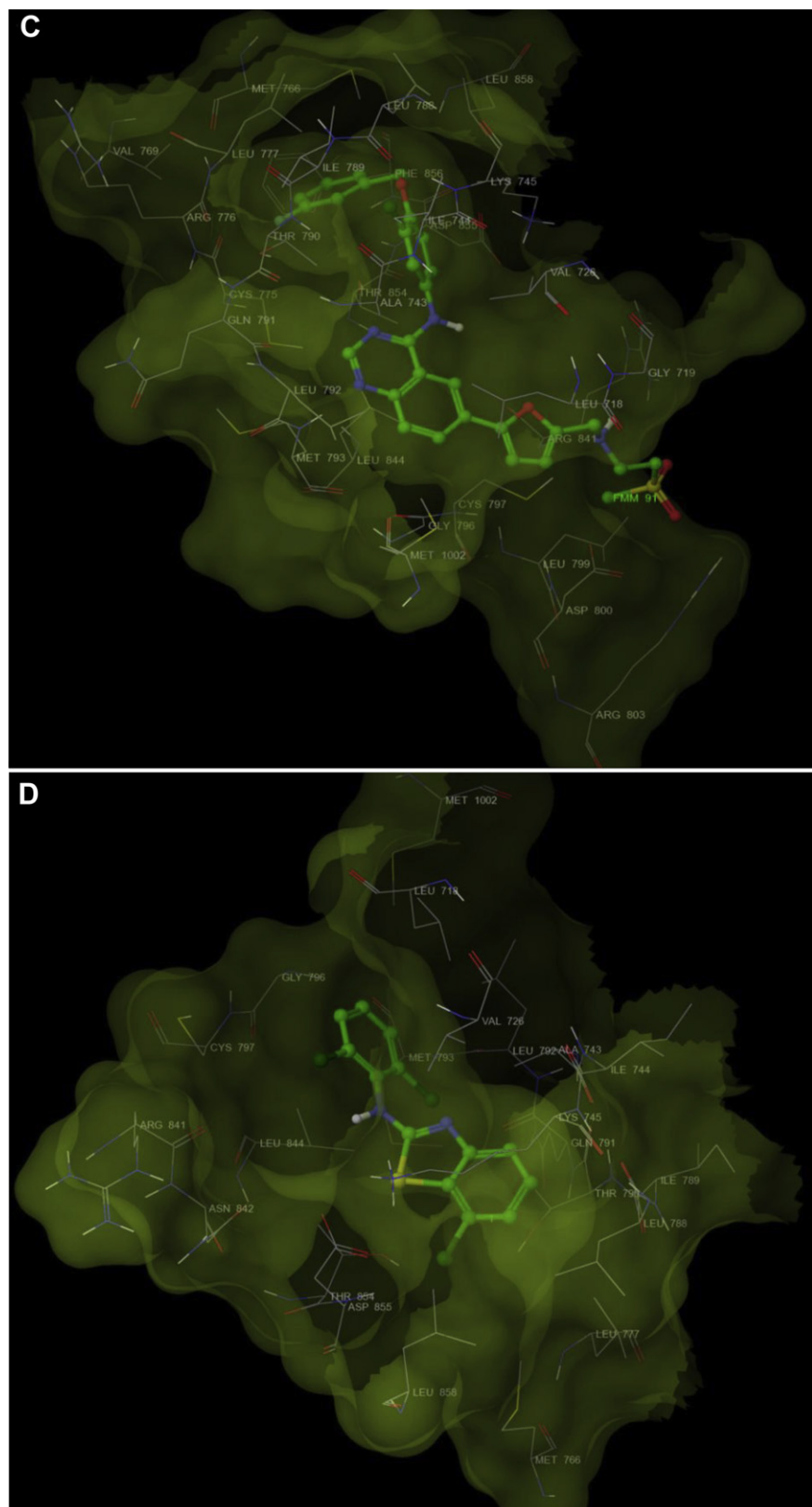


**Fig. 7.** Binding mode of **Lapatinib** (**C**) and compound **4i** (**D**) in the ATP binding site of EGFR-TK showing residue within 5 Å.







ligands using OPLS 2005 force field. The low energy conformation of the ligands was selected and was docked into the grid generated from protein structures using standard precision (SP) docking mode. The final evaluation is done with glide score (docking score) and single best pose is generated as the output for particular ligand.

## 7. Results and discussion

### 7.1. Pharmacophore modeling

The pharmacophore mapping was carried out to map the chemical features or functional groups present in the synthesized compounds which are essential for anticancer activity. We generated different pharmacophore pattern based on a set of synthesized aligned molecules. Selected pharmacophore shows five chemical features which were present in all the synthesized molecules (indicated by 100%) as shown in Fig. 5. The information shows that the five features used were two AroC feature (Aromatic), AliC feature (Aliphatic) one HDR (Hydrogen bond donor) features. The average RMSD of the pharmacophore alignment of each two molecule is 0.010511 Å. These five chemical features were found in all the synthesized molecules. The larger tessellated spheres are indicative of the common pharmacophore identified in the molecule. The smaller solid features are of the individual molecules. The common

pharmacophore having four larger orange color tessellated sphere shows aromatic and aliphatic carbon. Magneta color larger tessellated sphere shows the hydrogen bond donor as shown in Fig. 5. The distance among the various chemical features are as follows;

1. AroS (Benzothiazole) to AroC (Aniline) = 4.872 Å
2. AroS (Benzothiazole) to AliC (1st methyl of aniline) = 4.202 Å
3. AroS (Benzothiazole) to HDR (–NH–) = 5.392 Å
4. AroC (Aniline) to HDR (–NH–) = 5.351 Å
5. AroC (Aniline) to AliC (1st methyl of aniline) = 3.275 Å
6. HDR (–NH–) to AliC (1st methyl of aniline) = 3.621 Å
7. HDR (–NH–) to AliC (6th methyl of aniline) = 4.872 Å

Hypothesis generation was performed using low energy conformers of the molecules. All adapted models showed that the donor atoms of the NH fragments (magenta color larger tessellated) as hydrophilic element and the aryl moieties as hydrophobic element were well superimposed within the set distance tolerance. This confirms the important role of the hydrophilic and hydrophobic moieties for recognition and binding to receptor sites.

According to the pharmacophore generated by Molsign the minimal structural requirements for antitumor activity consist of an aromatic ring (hydrophobic region) attached to NH fragment (H-bonding donor region), and a hydrophobic region represented

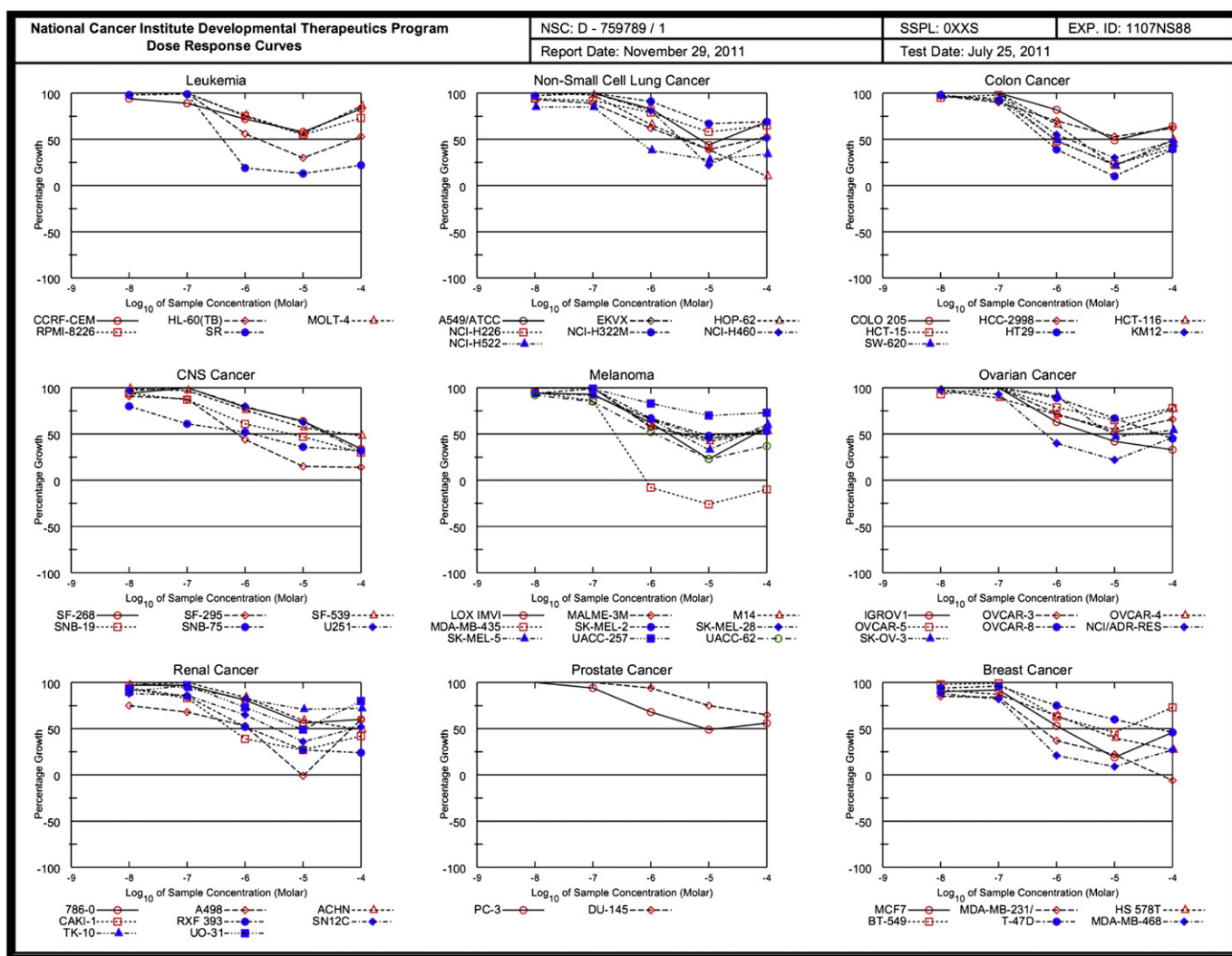


**Fig. 10.** Five dose assay graph of compound 4a (NSC: 105624/759789) against nine panel cancer cell line at NCI.





common residues involved in this type of interaction within 5 Å area are ALA-743, ARG-841, ASP-855, CYS-797, LEU-718, LEU-777, LEU-788, LYS-745, MET-766, THR-790 and THR-854 as shown in Table 2.

### 7.3. Primary single high dose ( $10^{-5}$ M) full NCI 60 cell panel *in vitro* assay

The tumor growth inhibition properties of the two compounds **4a** and **4i** with the NCI codes 105624/759789 and 105628/759390 selected among **4(a–j)** by the National Cancer Institute (NCI), USA, were screened on human tumor cell lines at single high dose ( $10^{-5}$  M) and five dose level at the NIH, Bethesda, Maryland, USA, under the drug discovery program of the NCI.

With regard to sensitivity against individual cell lines at primary single high dose ( $10^{-5}$  M). Compound **4a** showed remarkably lowest cell growth promotion against CNS cancer SNB-75 cell line and Melanoma MDA-MB-435 cancer cell line with cell growth promotion of –15.50 and –23.68 respectively as shown in Fig. 8. On the other hand compound **4i** was found to be broad spectrum against all nine panel of cancer cell line at primary single high dose ( $10^{-5}$  M) as shown in Fig. 11.

### 7.4. *In vitro* 5 dose full NCI 60 cell panel assay

All the cell lines (about 60), representing nine tumor subpanels, were incubated at five different concentrations (0.01, 0.1, 1, 10 & 100  $\mu$ M). The outcomes were used to create log concentration Vs % growth inhibition curves and three response parameters ( $GI_{50}$ , TGI and  $LC_{50}$ ) were calculated for each cell line. The  $GI_{50}$  value (growth inhibitory activity) corresponds to the concentration of the compound causing 50% decrease in net cell growth, the TGI value (cytostatic activity) is the concentration of the compound resulting in total growth inhibition and  $LC_{50}$  value (cytotoxic activity) is the concentration of the compound causing net 50% loss of initial cells at the end of the incubation period of 48 h [34–36].

Compound under investigation **4a** exhibited remarkable anti-cancer activity against most of the tested cell lines representing nine different subpanels with  $GI_{50}$  value  $4.12 \times 10^{-7}$  M against Leukemia SR cell line,  $5.52 \times 10^{-7}$  M against Non-Small Cell Lung Cancer NCI-H5222 cell line,  $9.20 \times 10^{-7}$  M,  $6.29 \times 10^{-7}$  M,  $9.47 \times 10^{-7}$  M against Colon Cancer HCT-116, HCT-15 and SW-620 cancer cell line respectively,  $7.25 \times 10^{-7}$  M against CNS cancer SF-295 cancer cell line,  $2.42 \times 10^{-7}$  M against Melanoma MDA-MB-435 cancer cell line,  $6.39 \times 10^{-7}$  M against Ovarian NCI/ADR-RES cancer cell line,  $5.64 \times 10^{-7}$  M against Renal Cancer CAKI-1

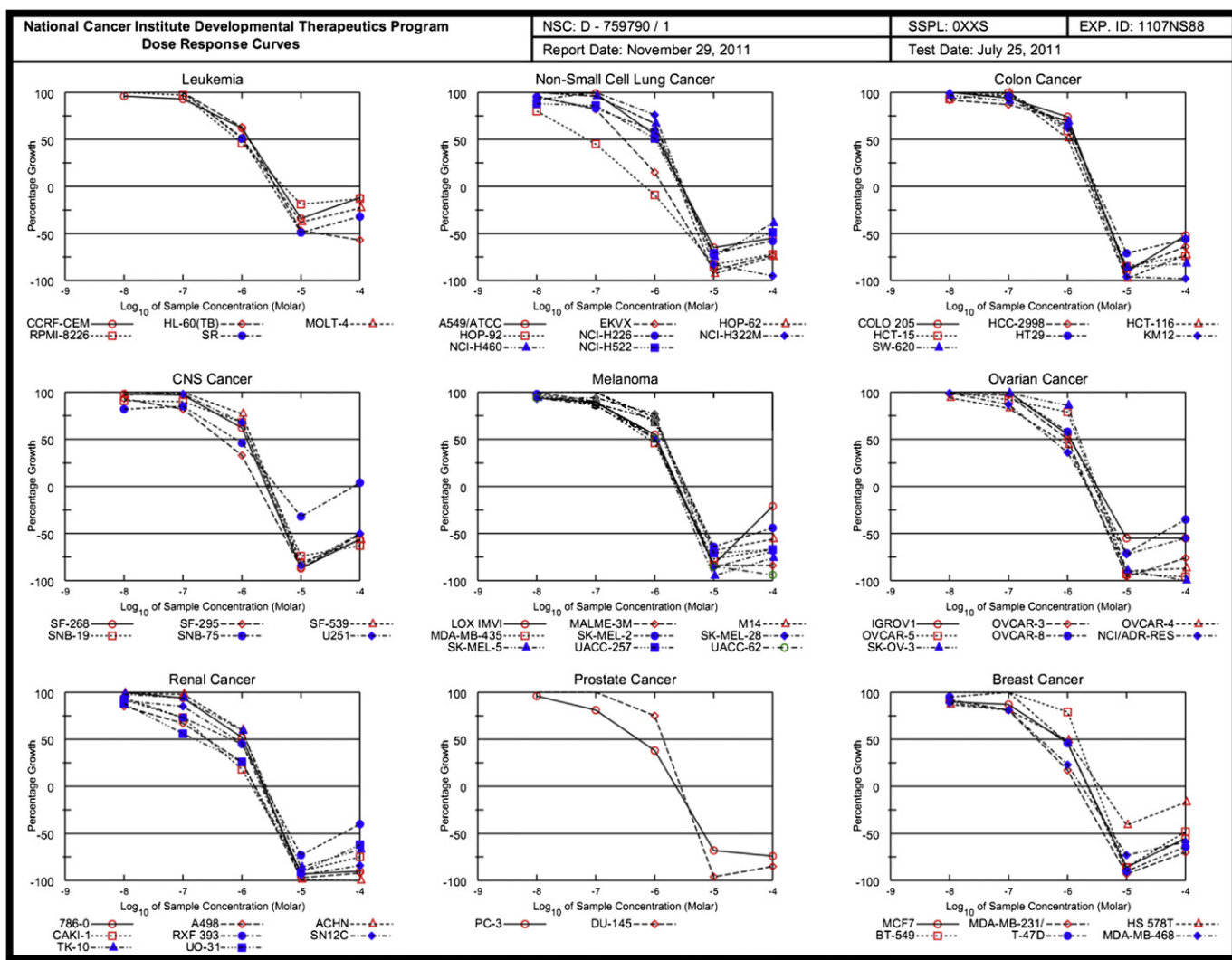


**Fig. 13.** Five dose assay graph of compound **4i** (NSC: 105628/759390) against nine panel of cancer cell line at NCI.



